Polycyclic Aromatic Hydrocarbons with Five-Membered Rings: Distributions within Isomer Families in Experiments and Computed Equilibria

Nathan D. Marsh and Mary J. Wornat*

Department of Mechanical and Aerospace Engineering, Princeton University, Princeton, New Jersey 08544

Received: June 13, 2002; In Final Form: February 5, 2004

Previous studies of polycyclic aromatic hydrocarbons (PAH) from a variety of combustion and pyrolysis systems have shown that certain aspects of the PAH product distribution, such as the relative abundance of certain isomers, are invariant over a range of fuels and reactor configurations. One possible explanation is that fast isomerization, facilitated by the presence of internal and external five-membered rings, may serve to normalize the product distributions, independent of the fuel or reactor configuration. To examine this possibility, we have compared experimentally measured PAH product distributions (within isomer families) to computed theoretical equilibrium distributions—first evaluating several quantum chemical methods for thermodynamic property computation: corrected AM1 semiempirical, HF/3-21G, B3LYP/STO-3G, and B3LYP/6-31G(d). Of the four methods, the corrected AM1 method is chosen for the equilibrium computations, since its root-mean-square deviation of the computed vibrational frequencies proves to be very close to that of the higher-order HF/3-21G method and since its computation is 100 times faster—a major consideration for the large molecules (3−9 rings) of this study. Using the corrected AM1 method, we have computed the Gibbs free energies and equilibrium distributions from 250 to 1500 K for the following sets of PAH isomers containing internally or externally fused five-membered rings: $C_{16}H_{10}$ = fluoranthene, aceanthrylene, and acephenanthrylene; $C_{18}H_{10}$ = cyclopent[*hi*]acephenanthrylene, cyclopenta[*cd*]fluoranthene, and benzo[*ghi*]fluoranthene; $C_{20}H_{10}$ = dicyclopenta[*cd,fg*]pyrene, dicyclopenta[*cd,jk*]pyrene, and dicyclopenta[*cd,mn*]pyrene; $C_{28}H_{12}$ = dicyclopenta[*bc,ef*]coronene, dicyclopenta[*bc,hi*]coronene, and dicyclopenta[*bc,kl*]coronene; $C_{20}H_{12}$ = benzo[*a*]fluoranthene, benzo[*b*]fluoranthene, benzo[*j*]fluoranthene, and benzo[*k*]fluoranthene; $C_{28}H_{16}$ = benzo[*a*]naphtho[2,3-*j*]fluoranthene, benzo[*a*]naphtho[2,3-*k*]fluoranthene, and benzo[*a*]naphtho[2,3-*l*]fluoranthene; $C_{13}H_{10}$ = fluorene, benz[*e*]indene, benz[*f*]indene, and benz[*g*]indene. Comparing the computed equilibrium distributions to those found experimentally in catechol (*o*-dihydroxybenzene) and anthracene pyrolysis products, we find close agreement only for the $C_{16}H_{10}$ isomers—corroborating previous evidence of a facile route for interconversion of internally and externally fused five-membered rings in this isomer group. Because $C_{16}H_{10}$ isomers are prominent among PAH in a wide range of pyrolysis and combustion systems, the investigation and incorporation (into PAH growth models) of $C_{16}H_{10}$ isomerization kinetics are very important. None of the other PAH isomer families investigated is found to exhibit such agreement between experimental and computed results, indicating that other isomerization mechanisms, such as ethylene migration around the PAH periphery or internal rearrangement of five-membered rings in fluoranthene benzologues, are of less significance over the time scales considered.

Introduction

Polycyclic aromatic hydrocarbons (PAH) are significant as constituents of combustion-generated pollutants, both because of their role as potential soot precursors[1,2] and because of the inherent biological activity of particular PAH.[3,4] In our investigation of the composition of combustion and pyrolysis products from a variety of fuels and reactor configurations,[5−16] we have identified a large number of PAH with internal and external five-membered rings, which are of particular interest because some of them appear to have enhanced biological activity, compared to benzenoid PAH.[3,17] Despite differences in parent fuel structures and in the physical environments in which PAH are produced, measured PAH product distributions from a variety of systems exhibit a number of similarities: within particular isomer groups, certain species are always dominant;[5−16] other species within an isomer family are never observed;[5−16] an increase in temperature or residence time enhances the yields of PAH with five-membered rings compared to those of benzenoid PAH.[5,6,8,15] Such trends are also observable from the data of other investigators who employ isomer-specific PAH measurement techniques.[1,2,18]

These similarities in PAH product distribution, observed across a broad range of experiments, may be explained if the PAH are formed via a limited set of significant reactions that occur mostly independent of fuel and reactor configuration. In fact, two canonical reactions for PAH formation and growth have been identified previously:[6,19−23] the Badger mechanism[24] for the union of an aryl radical to an aromatic molecule, and the hydrogen-abstraction/C_2-addition mechanism[25,26] for the addition of C_2 and subsequent ring closure. Isomerization reactions have also been suggested[6,17,27] to play a significant role in determining experimentally measured PAH product

* To whom correspondence should be addressed. Current address: Department of Chemical Engineering, Louisiana State University, South Stadium Drive, Baton Rouge, LA 70803. Tel: (225) 578-7509. Fax: (225) 578-1476. E-mail: mjwornat@lsu.edu.

10.1021/jp026319i CCC: $27.50
Published on Web 05/26/2004

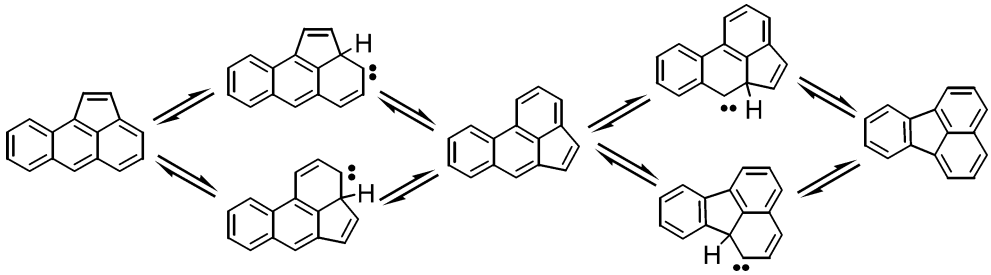

Figure 1. Unimolecular isomerization scheme for (from left to right) aceanthrylene, acephenanthrylene, and fluoranthene. Adapted from Scott and Roelofs[28] and Sarobe et al.[29]

distributions—in some cases[27] bringing about the production of more mutagenically active members within an isomer family.

A frequently invoked unimolecular isomerization for PAH under flash-vacuum pyrolysis conditions[28,29] is shown in Figure 1; however, its applicability to atmospheric pressure conditions frequently seen in combustion and pyrolysis environments is unknown. This scheme is significant in that the atomic rearrangement exploits the five-membered ring structure, a structure that occurs internally in the nonalternant PAH fluoranthene and externally in the cyclopenta-fused PAH aceanthrylene and acephenanthrylene. The scheme can, of course, easily be extended to include many other PAH that have been identified in combustion and pyrolysis products, so long as the conversion involves fluoranthene benzologues and cyclopenta-fused PAH.

Since the reactions depicted in Figure 1 are unimolecular, they may occur much more rapidly than bimolecular reactions, particularly in the dilute conditions often examined in flow reactors. However, kinetic rates for these reactions have not been determined, and doing so presents a significant computational challenge. Moreover, kinetic reaction paths for the isomerization of larger molecules have not yet been proposed, which significantly complicates a transition-state theory approach to kinetics. A simpler way to determine the significance of these reactions is to use thermodynamics to examine the upper bound for their rates (i.e., to suppose that the autoisomerization rates are significantly faster than those of bimolecular reactions, in which case the stable species may be considered to be in quasi-equilibrium). A further case for considering fast autoisomerization is that these species appear in similar isomer distributions across a wide range of fuels and reaction configurations, including products from flames. Although this work primarily focuses on pyrolysis reactions, the generally observed similarity between PAH distributions in combustion and pyrolysis systems suggests that the underlying chemistry is the same. For example, experiments in a well-stirred/plug-flow reactor[17] operating at equivalence ratios of 1.2 and 2.2 (implying the presence of oxygen atoms and radicals) show isomer ratios that are similar to those observed in pure pyrolysis experiments.[5,6,15]

In order to compute the equilibrium distributions that may result from fast isomerization reactions and compare these distributions with those found in experiments, it is necessary to determine the Gibbs free energy for each of the species in question. However, very little information exists on the thermodynamic properties of large PAH like those studied here—especially the novel cyclopenta-fused PAH, many of which have only recently become available for study due to the special syntheses[13,30] required. Our approach, therefore, is to compute from quantum theory the thermophysical properties (enthalpy and entropy) of these compounds, from which we then determine the Gibbs free energy for each species, across a range of temperatures. Recently, Pope et al.[31] have reported theoretical equilibrium distributions, computed via molecular mechanics methods, for four of the isomer families examined in this work, but they do not compare their results to distributions found in experiments, as we do here. Previously,[32] we have successfully utilized corrected semiempirical computations[33] to determine the heat of formation of large PAH. Although it is well established[34] that more computationally intensive methods such as density functional theory are more reliable than uncorrected semiempirical methods, corrected semiempirical methods—such as group correction of heat of formation[33] used in our previous work[32] and corrected vibrational frequencies[35] used for computing enthalpy and entropy—have not yet been extensively tested against the higher-level theories.

To make such an assessment in this work, we first examine a number of representative PAH having from one to six rings, comparing the computational expense and accuracy of several methods of property computation. We then use semiempirical quantum chemical computations with group correction to heats of formation, as well as corrected thermophysical properties, to determine the equilibrium distributions for selected isomer groups represented in our measured PAH product distributions.[5−16] Ranging in size from three to nine aromatic rings, the selected PAH contain at least one five-membered ring each and comprise the following sets of isomers: $C_{16}H_{10}$ = fluoranthene, aceanthrylene, and acephenanthrylene; $C_{18}H_{10}$ = cyclopent[*hi*]acephenanthrylene, cyclopenta[*cd*]fluoranthene, and benzo[*ghi*]fluoranthene; $C_{20}H_{10}$ = dicyclopenta[*cd,fg*]pyrene, dicyclopenta[*cd,jk*]pyrene, and dicyclopenta[*cd,mn*]pyrene; $C_{28}H_{12}$ = dicyclopenta[*bc,ef*]coronene, dicyclopenta[*bc,hi*]coronene, and dicyclopenta[*bc,kl*]coronene; $C_{20}H_{12}$ = benzo[*a*]fluoranthene, benzo[*b*]fluoranthene, benzo[*j*]fluoranthene, and benzo[*k*]fluoranthene; $C_{28}H_{16}$ = benzo[*a*]naphtho[2,3-*j*]fluoranthene, benzo[*a*]naphtho[2,3-*k*]fluoranthene, and benzo[*a*]naphtho[2,3-*l*]-fluoranthene; $C_{13}H_{10}$ = fluorene, benz[*e*]indene, benz[*f*]indene, and benz[*g*]indene. (The $C_{13}H_{10}$ isomer family is unique among those studied here in that its constituents are not fully aromatic, due to the saturated methylene carbon in each five-membered ring.)

Where appropriate, we compare the theoretical equilibrium distributions to the distributions determined from experiments, including the pyrolysis of catechol[15] (*o*-dihydroxybenzene) and anthracene.[5,6] In these experiments, the fuel is vaporized at a low concentration into an inert gas flow and then fed into electrically heated flow reactors held at uniform temperatures. The fuel undergoes pyrolysis for a known residence time (0.4 and 0.75 s for catechol and anthracene, respectively), at which point the gas is quenched and collected for further analysis. These residence times are relatively long in terms of kinetics, and therefore, the fast isomerization reactions proposed here should not be sensitive to the difference between the two sets of experiments. This, along with the low fuel concentration used, allows fast unimolecular (or inert-activated/deactivated) reac-

tions ample opportunity to establish equilibrium distributions in the experiments, if the reaction pathways exist.

Theoretical Approach

For the theoretical determination of each molecule's vibrational frequencies, the following computational methods are employed: a corrected AM1 semiempirical method, described below; the Hartree−Fock method with a 3-21G basis set; and the B3LYP density functional method,[36,37] with both the STO-3G and 6-31G(d) basis sets. Two important factors are considered in these methods: the computational time vs molecule size and the molecular root-mean-square (rms) error, similar to that defined by Scott and Radom,[34]

$$\mathrm{rms}_{\mathrm{mol}} = \left(\sum_{1}^{n_{\mathrm{mol}}} \Delta_{\mathrm{min}}/n_{\mathrm{mol}}\right)^{1/2}$$

where

$$\Delta_{\mathrm{min}} = (\omega_i^{\mathrm{theor}} - \omega_i^{\mathrm{B3LYP/6-31G(d)}})^2$$

This residual, Δ_{min}, differs slightly from the one of Scott and Radom, who compare the theoretical harmonic frequencies to experimental measurements for 122 molecules (1066 vibrational frequencies). Because experimental values are unavailable for the compounds examined in our work, the frequencies calculated by the widely used B3LYP/6-31G(d) method, considered by Scott and Radom one of the most effective in their study, are used as the reference for comparison. The value of $\mathrm{rms}_{\mathrm{mol}}$ is calculated for each of six compounds—benzene, naphthalene, acenaphthylene, acephenanthrylene, cyclopenta[*cd*]pyrene, and dicyclopenta[*cd,jk*]pyrene—and for each of three methods: corrected AM1, HF/3-21, and B3LYP/STO-3G. For the less computationally intensive methods (AM1 and B3LYP/STO-3G) computational times are found for four additional large molecules: coronene, benzo[*a*]naphtho[2,3-*j*]fluoranthene, cyclopenta[*bc*]coronene, and dicyclopenta[*bc,kl*]coronene. All computations are carried out on 500 MHz Pentium III systems using MOPAC[38] for the semiempirical calculations and Gaussian98[39] for the higher-level methods.

Because of the large number and sizes of species examined here, we compute properties using semiempirical quantum methods. Heats of formation are determined for all species using the AM1 Hamiltonian.[40] Wang and Frenklach[33] show that semiempirical computations introduce increasingly large errors as aromatic rings are added, resulting from approximations of the interatomic potential profile. This error is particularly problematic in the case of peripheral five-membered rings, a defining feature of the many cyclopenta-fused PAH we examine. For acenaphthylene, the simplest cyclopenta-fused PAH, the $\Delta_f H°$ is overpredicted by 25%. Fortunately, Wang and Frenklach[33] also show that these errors are systematic and can be corrected to within a few kilocalories for the species they study. Their method, used in this work, is similar to the group additivity method of Benson[41] but makes the improvement of using group characteristics for corrections to the computed $\Delta_f H°$, rather than simply summing group contributions to achieve the final value.

The very same approximation that introduces errors in the computation of heats of formation also introduces errors in the computation of other thermophysical properties, such as specific heat and entropy, necessary for the determination of equilibrium constants. To rectify these errors we use a somewhat more detailed method, also by Wang and Frenklach,[35] which computes thermophysical properties of molecules by summing the contributions of the rotational, translational, and corrected vibrational energy modes. (The rotational and translational components do not require correction because they depend only on temperature and, in the case of rotational entropy, on inertial moments and symmetry number—all of which can easily be determined with high accuracy.) Similar to the method used for heats of formation, corrected vibrational frequencies are calculated from the AM1 values and group corrections corresponding to structural units in the molecule. The corrected vibrational frequencies then allow the computation of the vibrational contribution to the property in question. This vibrational contribution is then combined with the rotational and translational contributions to yield the value of the property for a given temperature.

Once the corrected vibrational frequencies are obtained, therefore, Gibbs free energies can be computed for all species in question across a wide range of temperatures. Equilibrium constants may then be obtained, and therefore, equilibrium distributions of sets of isomers may be determined as a function of temperature.

Error Assesment. The error in the calculation of equilibrium distributions is estimated by examining their sensitivity to variations in the Gibbs free energies. For the molecules examined here, a variation of 1 kcal/mol in the Gibbs free energy of one of the isomers within the family results in an overall 10% variation in the equilibrium distribution. If other Gibbs energies have similar variations in the same direction (i.e., all positive or all negative), then the variation in the equilibrium distribution is less. In other words, in terms of error, the worst case is if the error in the Gibbs free energy is confined to only one of the isomers in the family.

The error in the Gibbs free energy is a consequence of errors in the calculations of entropy and heat of formation. In our previous work[32] we show a 1 kcal/mol difference between the corrected AM1 method and an ab initio computation of the heat of formation of pyracylene. Because of the highly strained (likely nonplanar) structure of pyracylene, as well as the pair of external five-membered rings, this molecule is more likely to reveal weaknesses in computational methods. Therefore, we expect the error in the heat of formation to be less than 1 kcal/mol for other molecules. The error in entropy is assessed by examining one of the test cases run at the B3LYP/6-31G(d) level as well as the corrected AM1. In that case, the maximum difference in Gibbs free energy between the two methods is 0.35 kcal/mol, with an average difference over the temperature range of 0.17 kcal/mol. Therefore, we expect that errors in heat of formation will dominate, in which case the equilibrium distributions are likely 10% off from those that would be calculated by the higher-level methods.

It is important to note that it is difficult to assess the error in the computed Gibbs free energies with reference to the true values for the molecules studied here, because they have never been measured. Instead, it is our purpose to compare the corrected AM1 method to the current "industry standard" B3LYP/6-31G(d) density functional method, in order to determine whether there is an unacceptable increase in error that accompanies the savings in computational time. However, it is worth noting that the B3LYP method has been tested on 122 molecules with known vibrational frequencies,[34] resulting in an rms error that corresponds to a 0.1 kcal/mol error in the Gibbs free energy. Furthermore, the B3LYP functional is believed to be robust and scaleable and, thus, applicable to larger molecules. It is, therefore, an appropriate benchmark against which other computational methods may be evaluated.

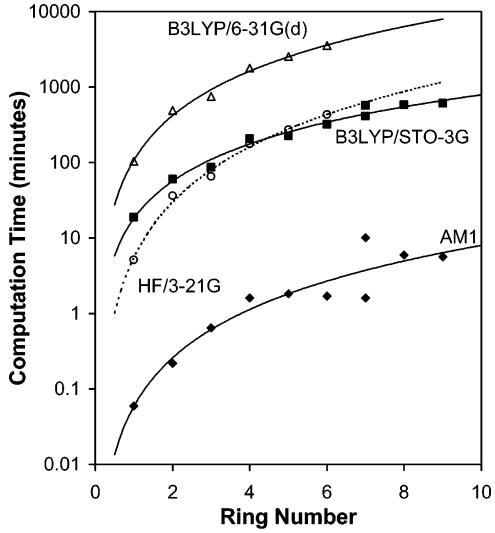

Figure 2. Time required for the computation of vibrational frequencies of PAH with one to seven rings, using the following methods: ◆ AM1 semiempirical; ○ HF/3-21G Hartree−Fock; ■ B3LYP/STO-3G density functional; △ B3LYP/6-31G(d) density functional.

TABLE 1: Root-Mean-Square Deviation from Frequencies Found by B3LYP/6-31G(d)

compound	no. of rings	rms_{mol} deviation (cm^{-1})		
		AM1	HF/3-21G	B3LYP/STO-3G
benzene	1	48	46	195
naphthalene	2	50	40	179
acenaphthylene	3	54	36	168
acephenanthrylene	4	53	37	164
cyclopenta[*cd*]pyrene	5	56	37	158
dicyclopenta[*cd*,*jk*]pyrene	6	58	35	152

Results and Discussion

Assessment of Computational Methods. Figure 2 shows the time, in minutes, required for the computation of an energy-minimized geometry and vibrational frequencies for the following representative PAH (in order of increasing ring number): benzene, naphthalene, acenaphthylene, acephenanthrylene, cyclopenta[*cd*]pyrene, dicyclopenta[*cd*,*jk*]pyrene, coronene and benzo[*a*]naphtho[2,3-*j*]fluoranthene, cyclopenta[*bc*]coronene, and dicyclopenta[*bc*,*kl*]coronene. As Figure 2 shows, the B3LYP/STO-3G and HF/3-21G methods are 100 times slower than the semiempirical AM1 method when computing geometry and vibrational frequencies; the B3LYP/6-31G(d) method is 1000 times slower than the AM1 method. It should be noted that the computational time for the AM1 method is computer time only; because it is relatively simple to automate, the time required to adjust the vibrational frequencies "by hand" is not considered.

Table 1 summarizes the rms_{mol} found for each molecule for each method. For reference, the rms_{ov} measured by Scott and Radom for the B3LYP/6-31G(d) method is 34 cm^{-1}. One significant finding from Table 1 is that the deviation of the other methods from the B3LYP/6-31G(d) results is not particularly dependent on molecular size or structure. In fact, there appears to be some convergence of the HF and the B3LYP/STO-3G results to the B3LYP/6-31G(d) results as molecule size increases. From the computed errors for each method, we determine that the AM1 semiempirical method is best suited for our application here. Significantly more time-intensive methods may produce slightly better or significantly worse results, depending primarily on the choice of basis set.

The corrected AM1 method (as described above) permits the computation of thermophysical properties, summarized in Table 2, which are used to determine the equilibrium distributions of PAH isomers.

Interconversion of Five- and Six-Membered Rings. Of primary interest to us are the PAH isomers containing five-membered rings—especially the $C_{16}H_{10}$ isomers, as they are the ones originally proposed[28] to have an explicit isomerization route. The computed equilibrium distribution of isomers of the $C_{16}H_{10}$ family (fluoranthene, aceanthrylene, and acephenanthrylene) is shown in Figure 3, along with the fractions measured

TABLE 2: Thermophysical Properties of PAH Isomers, as Computed by the Corrected AM1 Method

compound	$\Delta_f H°_{298}$ (kcal/mol)	$S°_{298}$ (cal/mol/K)	C_{p300} (cal/mol/K)	C_{p500} (cal/mol/K)	C_{p700} (cal/mol/K)	C_{p1000} (cal/mol/K)	C_{p1500} (cal/mol/K)
fluroanthene	69.2	94.53	48.75	78.98	98.97	117.07	132.29
acephenanthrylene	73.9	95.99	48.78	79.01	98.98	117.05	132.25
aceanthrylene	81.5	96.10	48.97	79.13	99.05	117.09	132.27
pyrene	53.9	98.00	48.30	78.52	98.61	116.86	132.19
cyclopenta[*cd*]fluoranthene	107.9	99.08	53.64	86.65	108.21	127.50	143.50
cyclopent[*hi*]acephenanthrylene	97.5	98.17	53.64	86.63	108.18	127.45	143.45
benzo[*ghi*]fluoranthene	98.8	97.68	53.14	86.18	107.88	127.34	143.46
cyclopenta[*cd*]pyrene	82.0	98.08	53.15	86.19	107.87	127.30	143.41
dicyclopenta[*cd*,*fg*]pyrene	111.0	108.39	58.04	93.84	117.08	137.71	154.61
dicyclopenta[*cd*,*jk*]pyrene	113.4	108.60	58.08	93.91	117.14	137.74	154.63
dicyclopenta[*cd*,*mn*]pyrene	117.2	109.47	58.15	93.94	117.16	137.76	154.64
dicyclopenta[*bc*,*ef*]coronene	127.5	128.28	78.91	127.29	158.71	186.31	208.51
dicyclopenta[*bc*,*hi*]coronene	128.2	128.17	78.94	127.35	158.76	186.34	208.52
dicyclopenta[*bc*,*kl*]coronene	126.9	125.66	78.66	127.14	158.60	186.23	208.46
benzo[*a*]fluoranthene	89.2	116.23	61.10	98.36	123.03	145.32	163.97
benzo[*b*]fluoranthene	81.0	115.83	60.89	98.24	122.97	145.29	163.96
benzo[*j*]fluoranthene	86.9	116.29	60.97	98.28	122.98	145.30	163.96
benzo[*k*]fluoranthene	83.0	114.31	60.89	98.24	122.94	145.26	163.94
benzo[*a*]naphtho[2,3-*j*]fluoranthene	128.1	126.39	83.61	135.06	169.12	199.81	225.34
benzo[*a*]naphtho[2,3-*k*]fluoranthene	122.9	121.78	81.64	133.08	167.11	197.80	223.33
benzo[*a*]naphtho[2,3-*l*]fluoranthene	132.6	124.74	83.17	134.87	169.05	199.81	225.36
benz[*e*]indene	53.9	94.87	41.37	67.65	85.30	101.53	115.49
benz[*f*]indene	53.9	94.86	41.36	67.62	85.26	101.50	115.47
benz[*g*]indene	53.9	94.89	41.39	67.67	85.31	101.54	115.50
fluorene	45.0	93.51	41.21	67.56	85.27	101.55	115.53

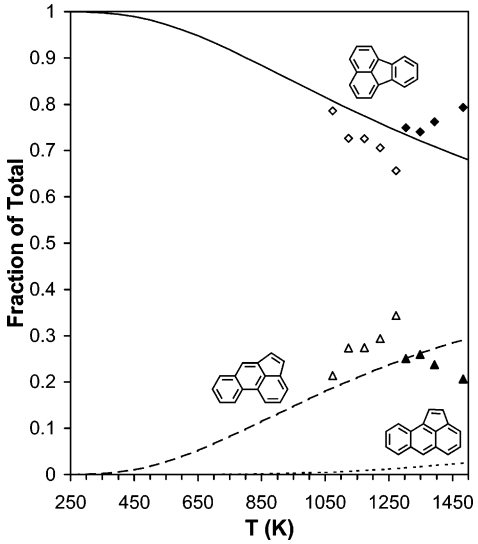

Figure 3. Computed equilibrium distribution and experimental measurements of the $C_{16}H_{10}$ isomers: fluoranthene (solid line and ◇,◆), acephenanthrylene (dashed line and △,▲), and aceanthrylene (dotted line). Experimental data from catechol pyrolysis[15] (open symbols) and anthracene pyrolysis[5,6] (closed symbols).

in the products of flow-reactor pyrolysis of catechol[15] and drop-tube pyrolysis of anthracene.[6] (Accurate quantification of the $C_{16}H_{10}$ isomer aceanthrylene in the experiments is difficult because it co-elutes with the $C_{16}H_{10}$ isomer fluoranthene.[6,15] Consequently, Figure 3 does not show the experimental fraction of aceanthrylene. Spectroscopic evidence,[6,11] however, reveals that in the experiments, aceanthrylene is present in much smaller quantities than fluoranthene—a trend also exhibited by the computed equilibrium distribution in Figure 3.) From Figure 3, it can be seen that experimentally measured yields of fluoranthene and acephenanthrylene come very close to the theoretical equilibrium values. In the case of the catechol products, indicated by the open symbols, the distribution is slightly inside the theoretical equilibrium, but the trend moves in the appropriate direction as temperature increases. In the case of the anthracene products, indicated by closed symbols, the distribution is almost identical to theoretical equilibrium at the lower temperatures of these experiments. As temperature increases, however, the experimental values show some departure from the equilibrium profiles. The departure falls within the expected error in the equilibrium distribution, but it is also possible that a fast high-temperature channel exists that competes with the isomerization reactions. That the experimental data match the theoretical distribution so well indicates that fast isomerization routes between these three isomers must be considered.

We have also examined the benzenoid $C_{16}H_{10}$ isomer pyrene, which contains only six-membered rings and does not have any obvious isomerization paths from fluoranthene or the $C_{16}H_{10}$ cyclopenta-fused PAH. When we consider the calculated equilibrium distribution of pyrene (not shown) with respect to the other three $C_{16}H_{10}$ isomers, we find that pyrene completely dominates the distribution by several orders of magnitude. However, experimental results from atmospheric-pressure studies of numerous fuels[6,7,10−12,14,15] show pyrene always to be in lower quantities than fluoranthene. Clearly, pyrene does not exist in any kind of equilibrium state with the other three $C_{16}H_{10}$ isomers in any atmospheric-pressure systems that we have examined. Furthermore, we can make the stronger statement that any reactions that allow pyrene to convert to the other three $C_{16}H_{10}$ isomers (including multistep and multibody reactions)

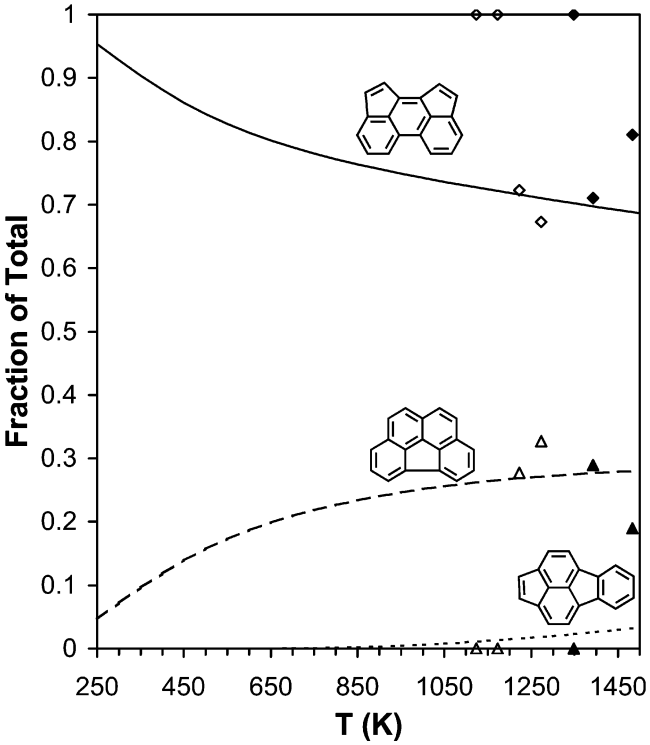

Figure 4. Computed equilibrium distribution and experimental measurements of the $C_{18}H_{10}$ isomers: cyclopent[*hi*]acephenanthrylene (solid line and ◇,◆), benzo[*ghi*]fluoranthene (dashed line), and cyclopenta[*cd*]fluoranthene (dotted line and △,▲). Experimental data from catechol pyrolysis[15] (open symbols) and anthracene pyrolysis[5,6] (closed symbols).

must be relatively slow compared to other formation and destruction reactions involving these species.

In contrast to the $C_{16}H_{10}$ isomers of Figure 3, the $C_{18}H_{10}$ isomers cyclopent[*hi*]acephenanthrylene, benzo[*ghi*]fluoranthene, and cyclopenta[*cd*]fluoranthene, whose equilibrium and experimental distributions are shown in Figure 4, do not, in experiment, follow the equilibrium trend determined by theory. Although cyclopent[*hi*]acephenanthrylene is the most abundant isomer in both experimental and theoretical distribution, the other isomers do not follow equilibrium behavior in any way. In particular, although benzo[*ghi*]fluoranthene is predicted to appear in moderate quantities relative to cyclopent[*hi*]acephenanthrylene, and in much larger quantities than cyclopenta[*cd*]-fluoranthene, in experiment benzo[*ghi*]fluoranthene proves very difficult to detect. In general, it is not found in significant quantities in systems where cyclopenta-fused PAH are abundant.[2] The evaluation of the experimental distribution of the $C_{18}H_{10}$ isomers is further complicated by the fact that they are found in relatively small quantities, such that the less abundant cyclopenta[*cd*]fluoranthene is not quantifiable in the catechol experiments below 1223 K, and is also not quantified in the lowest-temperature anthracene pyrolysis products. Despite the difficulty in quantifying experimental results, it is evident that these three isomers do not have an equilibrium distribution in these experiments. Furthermore, as with the $C_{16}H_{10}$ isomers, a fourth observed $C_{18}H_{10}$ isomer, cyclopenta[*cd*]pyrene, completely dominates the computed equilibrium distribution if it is included. Unlike the $C_{16}H_{10}$ case, however, this result is more consistent with experimental results. In catechol[15] and anthracene[5,6] products, cyclopenta[*cd*]pyrene usually appears in nearly 10 times the yield of the next most abundant isomer, cyclopent[*hi*]acephenanthrylene.

External Five-Membered Rings—Perimeter Migration. Another group of isomers which might have a specific isomer-

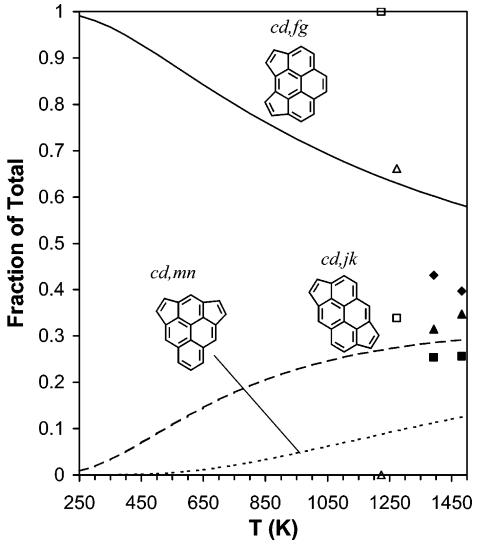

Figure 5. Computed equilibrium distribution and experimental measurements of the $C_{20}H_{10}$ isomers: "ortho" dicyclopenta[*cd,fg*]pyrene (solid line and ◆), "para" dicyclopenta[*cd,jk*]pyrene (dashed line and □,■), and "meta" dicyclopenta[*cd,mn*]pyrene (dotted line and △,▲). Experimental data from catechol pyrolysis[15] (open symbols) and anthracene pyrolysis[5,6] (closed symbols).

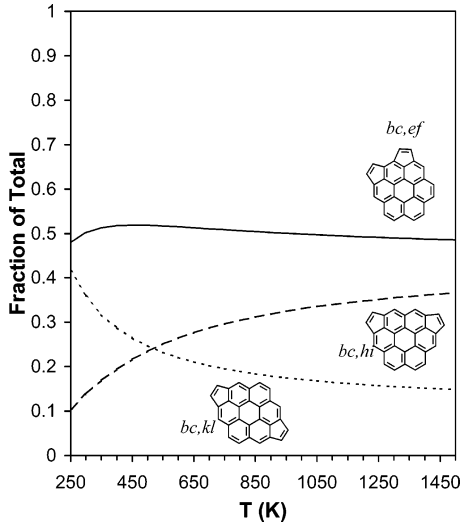

Figure 6. Computed equilibrium distribution of the $C_{28}H_{12}$ isomers: "ortho" dicyclopenta[*bc,ef*]coronene (solid line), "meta" dicyclopenta[*bc,hi*]coronene (dashed line), and "para" dicyclopenta[*bc,kl*]coronene (dotted line).

ization mechanism attributed to them are the three $C_{20}H_{10}$ dicyclopentapyrene isomers; it has been suggested that the ethylene bridge which forms the five-membered rings might have some mobility about the perimeter of PAH structures.[42−44] Therefore, we also examine the equilibrium distributions of the three dicyclopentapyrenes, shown in Figure 5. In experiments where only a single dicyclopentapyrene is observed,[6,15] as in the 1223 K catechol products, it is dicyclopenta[*cd,jk*]pyrene, the "para" isomer, corresponding to the middle curve in Figure 5. When a second dicyclopentapyrene is present,[8,15] as in the 1273 K catechol pyrolysis products, it is dicyclopenta[*cd,mn*]-pyrene, the "meta" isomer, corresponding to the bottom curve in Figure 5. The "ortho" isomer, dicyclopenta[*cd,fg*]pyrene, corresponding to the top curve in Figure 5, is only observed in the anthracene products,[5] although in that case it is the most prevalent dicyclopentapyrene. Furthermore, when dicyclopenta-[*cd,mn*]pyrene is present, it is often present in larger quantities than dicyclopenta[*cd,jk*]pyrene. In summary, the computed equilibrium distribution is not consistent with observations from experiments, so we conclude that the dicyclopentapyrenes do not isomerize among one another faster than they are formed and destroyed in other reactions.

The largest cyclopenta-fused PAH examined here, the $C_{28}H_{12}$ dicyclopentacoronenes, are similar to the dicyclopentapyrenes, in that there are three isomers differentiated by the relative locations of the two externally fused five-membered rings, and that there is the possibility[42−44] for these rings to migrate around the molecule. Despite their large size and novelty, these compounds have been observed[16] in anthracene pyrolysis products[5,6] as well as those from an ethylene flat flame, from a benzene flat flame, and from fuel-rich ethylene combustion in a jet-stirred/plug-flow reactor. (Descriptions of the equipment and methods for the latter three systems can be found in the literature.[1,45,46]) As in the case of the dicyclopentapyrenes, we find that in the equilibrium distribution of the dicyclopenta-coronenes, shown in Figure 6, it is the "ortho" isomer which is most abundant. However, the calculated equilibrium distribution of the dicyclopentacoronenes differs from that of the dicyclo-pentapyrenes in several ways. First, the fraction of dicyclopenta-[*bc,ef*]coronene, the "ortho" isomer, barely rises above 0.5, while the fraction of dicyclopenta[*cd,fg*]pyrene (the "ortho" isomer shown in Figure 5) never falls below 0.5. Second, except at the lowest temperatures, the second most prevalent dicyclopenta-coronene is the "meta" isomer (Figure 6); among the dicyclo-pentapyrenes, the "meta" isomer is by far the lowest yield, never rising above 10%. In the anthracene pyrolysis products, dicy-clopenta[*bc,kl*]coronene and dicyclopenta[*bc,hi*]coronene (the "meta" and "para" isomers) have comparable yields. Because a reference standard of dicyclopenta[*bc,ef*]coronene is not available, its presence must be inferred from chromatographic and mass spectral evidence;[16] the peak believed to be dicyclo-penta[*bc,ef*]coronene (the "ortho" isomer) is of significantly smaller size than those of the two identified isomers. These observations thus suggest that the relative levels of the dicy-clopentacoronenes in the experiments do not constitute an equilibrium distribution—a result similar to that for the dicy-clopentapyrenes.

Internal Five-Membered Rings—Fluoranthene Benzo-logues. Like cyclopenta-fused PAH, fluoranthene benzologues also may have the opportunity to isomerize among one another, although the detailed chemistry is not obvious. Two $C_{20}H_{12}$ fluoranthene benzologues, benzo[*j*]- and benzo[*k*]fluoranthene, are structurally similar in that they are both a pair of naphthalene units joined by a five-membered ring; a "rotation" of one of the naphthalene units could account for their interconversion. The computed equilibrium distribution of the benzofluoranthene isomers, shown in Figure 7, in fact shows the dominance of a single isomer, benzo[*b*]fluoranthene, which decreases somewhat with increasing temperature. This trend is also found in the catechol pyrolysis experiments, although the fraction of benzo-[*b*]fluoranthene is significantly less than in the computed equilibrium distribution. Figure 7 also reveals that in the catechol pyrolysis products benzo[*j*]fluoranthene is the second most abundant and benzo[*k*]fluoranthene falls a close third, whereas in the computed equilibrium distribution, the order of these two compounds is reversed. It should also be noted that at 1227 K only, benzo[*k*]fluoranthene is more prevalent in the catechol pyrolysis products than benzo[*j*]fluoranthene, a result of a sharper peak in the yield/temperature profile of benzo[*k*]-fluoranthene.[15] The least abundant isomer, by both computation and experiment, is benzo[*a*]fluoranthene, which has been identified in the products of catechol pyrolysis[11] but has not

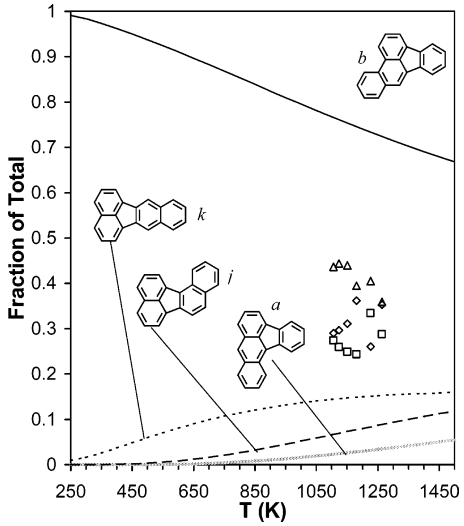

Figure 7. Computed equilibrium distribution and experimental measurements of the $C_{20}H_{12}$ isomers: benzo[*b*]fluoranthene (solid line and △), benzo[*j*]fluoranthene (dashed line and ◇), benzo[*k*]fluoranthene (dotted line and □), and benzo[*a*]fluoranthene (gray line). Experimental data (open symbols) from catechol pyrolysis.[15]

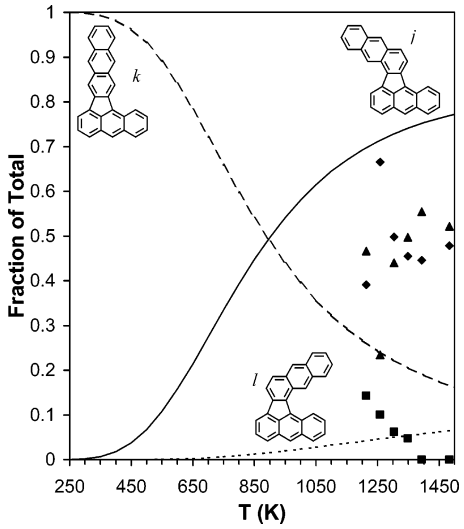

Figure 8. Computed equilibrium distribution of the $C_{28}H_{16}$ isomers: benzo[*a*]naphtho[*2,3-j*]fluoranthene (solid line and ◆), benzo[*a*]naphtho[*2,3-k*]fluoranthene (dashed line and ▲), and benzo[*a*]naphtho[*2,3-l*]fluoranthene (dotted line and ■). Experimental data (closed symbols) from anthracene pyrolysis.[5,6]

been quantified because its yield is too small. A comparison of the overall computed equilibrium distribution to that displayed by the catechol pyrolysis experiments shows that, despite the correct prediction of the most abundant isomer, the experimentally observed benzofluoranthene product distribution is not consistent with an equilibrium distribution.

Another set of isomers among the fluoranthene benzologues are the $C_{28}H_{16}$ benzonaphthofluoranthenes. These compounds, found in the products of anthracene pyrolysis, apparently result[6,47] from cyclodehydrogenation of the bianthryls, which are abundantly produced during anthracene pyrolysis.[6,47,48] As with benzo[*j*]- and benzo[*k*]fluoranthene, the internal five-membered ring in each benzonaphthofluoranthene may facilitate atomic rearrangement by allowing a "rotation" of one of the anthracene units. Figure 8, the distribution plot for the benzonaphthofluoranthenes, reveals a unique feature in the computed equilibrium distribution for this isomer set: it is the only one examined in which the dominant compound changes with

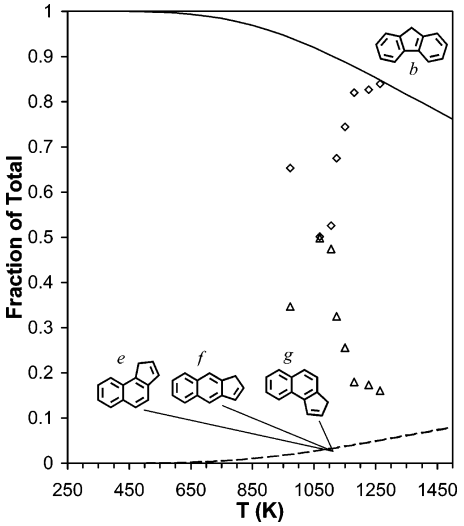

Figure 9. Computed equilibrium distribution of the $C_{13}H_{10}$ isomers: benz[*b*]indene (fluorene) (solid line and ◇), benz[*f*]indene (dashed line and △), benz[*e*]indene (dotted line), and benz[*g*]indene (dash/dot line). Experimental data (open symbols) from catechol pyrolysis.[15]

temperature. According to the calculations, at the lower temperatures, the "*k*" isomer is the most dominant; at the higher temperatures the "*j*" isomer is. At all temperatures, the "*l*" isomer is the least abundant, both in the computed equilibrium distribution and in the anthracene pyrolysis experiments. However, the experimental distribution of the two primary isomers does not agree with the equilibrium distribution, as these isomers are measured in similar quantities in the temperature range of the anthracene experiments. (It is worth noting that the computed equilibrium distribution predicts equivalent levels of the "*j*" and "*k*" isomers at temperatures just under 900 K, lower than the temperatures of the experiments. Within the temperature range of the experiments, the computed equilibrium distribution clearly indicates a preference for the "*j*" isomer.)

Methylene Carbon Rings—Indene Benzologues. Figure 9 displays the computational and experimental results for the $C_{13}H_{10}$ benzindenes—each of which contains a methylene carbon, distinguishing this isomer group from the cyclopenta-fused PAH and the fluoranthene benzologues examined above. Figure 9 reveals a qualitative consistency between the theoretical and experimental results: both the equilibrium calculations and the experimental catechol product data show fluorene (benz[*b*]-indene) to be the most abundant benzindene isomer. However, only at temperatures >1160 K do the theoretical and experimental results show fair quantitative agreement for benz[*b*]-indene and benz[*f*]indene. The equilibrium calculations predict the other two isomers, benz[*e*]indene and benz[*g*]indene, to be present at levels virtually identical to those of benz[*f*]indene. Neither the "*e*" nor "*g*" isomer has ever been shown to be in fuel products, however—to our knowledge, no reference standard of either exists[7] that would permit us to be certain whether these isomers are present in our catechol pyrolysis products. What we can say with assurance is that if either of these isomers is present at all, it is at a level significantly lower than that of benz[*f*]indene, since there are no large unidentified peaks or interfering spectra (with elution times appropriate to benzindenes) in the catechol product chromatograms.[11] In general, the experimental product distributions of the $C_{13}H_{10}$ isomers are not consistent with the equilibrium calculations in Figure 9, indicating that it is unlikely that the $C_{13}H_{10}$ benzindenes are prone to rapid isomerization.

Conclusions

We have considered several families of PAH isomers to determine their theoretical equilibrium distributions. After surveying several quantum chemical computational methods, it is clear that corrected semiempirical computations are only somewhat less accurate than higher-level methods, yet they are 100−1000 times faster than the other methods considered. Although more accurate and computationally expensive methods are certainly appropriate for small molecules, for the purposes of examining large PAH, as in this work, the corrected AM1 semiempirical method is the best choice. Therefore this method is used to compute (corrected) heats of formation and vibrational frequencies, which themselves are used to compute thermophysical properties and ultimately equilibrium constants for a number of PAH isomer groups. Of particular focus in this work are the PAH with five-membered rings—including cyclopenta-fused PAH, fluoranthene benzologues, and PAH with methylene carbons.

In the case of the $C_{16}H_{10}$ isomers fluoranthene, aceanthrylene, and acephenanthrylene, the equilibrium distribution seems to reflect the general behavior of these compounds as observed in experiments—with respect to both overall distribution and temperature effects. It is therefore critical that future studies of PAH kinetics consider unimolecular isomerization between these three compounds. Furthermore, there is an additional $C_{16}H_{10}$ isomer, the benzenoid PAH pyrene, which is not only not in equilibrium with the other isomers, but whose formation and destruction may only be linked to the other isomers by relatively slow reactions.

For the other isomer groups considered ($C_{18}H_{10}$, $C_{20}H_{10}$, $C_{28}H_{12}$, $C_{20}H_{12}$, $C_{28}H_{16}$, and $C_{13}H_{10}$), there is no evidence that equilibrium distributions are observed in experiments. In some cases, such as the $C_{20}H_{12}$ benzofluoranthenes or the $C_{13}H_{10}$ benzindenes, the data clearly indicate that the distribution seen in experiment is explicitly not the equilibrium distribution. Furthermore, there are particular PAH (such as pyrene and cyclopenta[*cd*]pyrene) that may form in parallel to their isomers, but clearly do not isomerize at a significant rate because the theoretical equilibrium predicts their dominance by several orders of magnitude, a result counter to that observed in experiments.

In developing PAH growth models, therefore, it is critical that the kinetics for the isomerization of the $C_{16}H_{10}$ isomers fluoranthene, aceanthrylene, and acephenanthrylene be investigated and incorporated in detail. In particular, this family of PAH provides a facile route between internally and externally fused five-membered rings, which may have an effect on the general nature of PAH distributions from a variety of fuels and reaction configurations. On the other hand, external five-membered rings do not appear to be particularly mobile around the PAH periphery because the compounds where this mobility might be most easily observed, the dicyclopentapyrenes and the dicyclopentacoronenes, do not follow the equilibrium distribution in experiment. Furthermore, an internal five-membered ring does not appear to aid rearrangement into other compounds with internal five-membered rings, as the fluoranthene benzologues do not follow the equilibrium distribution in experiment. Therefore these kinds of rearrangements are not as critical for inclusion in PAH mechanisms as is the $C_{16}H_{10}$ isomerization.

Acknowledgment. The authors gratefully acknowledge the National Science Foundation and Philip Morris, Inc., for financial support of portions of this work.

References and Notes

(1) Benish, T. G.; Lafleur, A. L.; Taghizadeh, K.; Howard, J. B. *Proc. Combust. Inst.* **1996**, *26*, 2319.

(2) Lafleur, A. L.; Howard, J. B.; Taghizadeh, K.; Plummer, E. F.; Scott, L. T.; Necula, A.; Swallow, K. C. *J. Phys. Chem.* **1996**, *100*, 17421.

(3) Durant, J. L.; Busby, W. F.; Lafleur, A. L.; Penman, B. W.; Crespi, C. L. *Mutat. Res.* **1996**, *371*, 123.

(4) Durant, J. L.; Lafleur, A. L.; Busby, W. F.; Donhoffner, L. L.; Penman, B. W.; Crespi, C. L. *Mutat. Res.* **1999**, *446*, 1.

(5) Wornat, M. J.; Vriesendorp, F. J. J.; Lafleur, A. L.; Plummer, E. F.; Necula, A.; Scott, L. T. *Polycyclic Aromat. Compd.* **1999**, *13*, 221.

(6) Wornat, M. J.; Sarofim, A. F.; Lafleur, A. L. *Proc. Combust. Inst.* **1992**, *24*, 955.

(7) Wornat, M. J.; Mikolajczak, C. J.; Vernaglia, B. A.; Kalish, M. A. *Energy Fuels* **1999**, *13*, 1092.

(8) Wornat, M. J.; Vernaglia, B. A.; Lafleur, A. L.; Plummer, E. F.; Taghizadeh, K.; Nelson, P. F.; Li, C.-Z.; Necula, A.; Scott, L. T. *Proc. Combust. Inst.* **1998**, *27*, 1677.

(9) Ledesma, E. B.; Kalish, M. A.; Wornat, M. J.; Nelson, P. F.; Mackie, J. C. *Energy Fuels* **1999**, *13*, 1167.

(10) Ledesma, E. B.; Kalish, M. A.; Nelson, P. F.; Wornat, M. J.; Mackie, J. C. *Fuel* **2000**, *79*, 1801.

(11) Wornat, M. J.; Ledesma, E. B.; Marsh, N. D. *Fuel* **2001**, *80*, 1711.

(12) Marsh, N. D.; Zhu, D.; Wornat, M. J. *Proc. Combust. Inst.* **1998**, *27*, 1897.

(13) Marsh, N. D.; Wornat, M. J.; Scott, L. T.; Necula, A.; Lafleur, A. L.; Plummer, E. F. *Polycyclic Aromat. Compd.* **1999**, *13*, 379.

(14) Wornat, M. J.; Ledesma, E. B.; Sandrowitz, A. K.; Roth, M. J.; Dawsey, S. M.; Qiao, Y. L.; Chen, W. *Environ. Sci. Technol.* **2001**, *35*, 1943.

(15) Marsh, N. D.; Ledesma, E. B.; Sandrowitz, A. K.; Wornat, M. J. *Energy Fuels* **2004**, *18*, 209.

(16) Wornat, M. J.; Vriesendorp, F. J. J.; Necula, A.; Scott, L. T.; Lafleur, A. L.; Plummer, E. F.; Taghizadeh, K.; Swallow, K. C. "The Identification of Two New $C_{28}H_{12}$ Dicyclopenta-Fused Polycyclic Aromatic Hydrocarbons in the Pyrolysis and Combustion Products of a Variety of Fuels"; Seventeenth International Symposium on Polycyclic Aromatic Compounds, 1999, Bordeaux, France.

(17) Howard, J. B.; Longwell, J. P.; Marr, J. A.; Pope, C. J.; Busby, W. F.; Lafleur, A. L.; Taghizadeh, K. *Combust. Flame* **1995**, *101*, 262.

(18) Lafleur, A. L.; Howard, J. B.; Plummer, E.; Taghizadeh, K.; Necula, A.; Scott, L. T.; Swallow, K. C. *Polycyclic Aromat. Compd.* **1998**, *12*, 223.

(19) Richter, H.; Grieco, W. J.; Howard, J. B. *Combust. Flame* **1999**, *119*, 1.

(20) Wang, H.; Frenklach, M. *Combust. Flame* **1997**, *110*, 173.

(21) Richter, H.; Mazyar, O. A.; Sumathi, R.; Green, W. H.; Howard, J. B.; Bozzelli, J. W. *J. Phys. Chem. A* **2001**, *105*, 1561.

(22) Wornat, M. J.; Sarofim, A. F.; Longwell, J. P. *Proc. Combust. Inst.* **1988**, *22*, 135.

(23) Masonjones, M. C.; Sarofim, A. F.; Lafleur, A. L. *Polycyclic Aromat. Compd.* **1996**, *8*, 23.

(24) Badger, G. M. *Prog. Phys. Org. Chem.* **1965**, *3*, 1.

(25) Bockhorn, H.; Fetting, F.; Wenz, H. W. *Ber. Bunsen−Ges. Phys. Chem.* **1983**, *87*, 1067.

(26) Frenklach, M.; Clary, D. W.; Gardiner, W. C. J.; Stein, S. E. *Proc. Combust. Inst.* **1984**, *20*, 887.

(27) Masonjones, M. C.; Lafleur, A. L.; Sarofim, A. F. *Combust. Sci. Technol.* **1995**, *109*, 273.

(28) Scott, L. T.; Roelofs, N. H. *J. Am. Chem. Soc.* **1987**, *109*, 5461.

(29) Sarobe, M.; Jenneskens, L. W.; Wesseling, J.; Snoeijer, J. D.; Zwikker, J. W.; Wiersum, U. E. *Liebigs Ann./Recl.* **1997**, 1207.

(30) Scott, L. T.; Necula, A. *J. Org. Chem.* **1996**, *61*, 386.

(31) Pope, C. J.; Peters, W. A.; Howard, J. B. *J. Hazard. Mater.* **2000**, *79*, 189.

(32) Marsh, N. D.; Wornat, M. J. *Proc. Combust. Inst.* **2000**, *28*, 2585.

(33) Wang, H.; Frenklach, M. *J. Phys. Chem.* **1993**, *97*, 3867.

(34) Scott, A. P.; Radom, L. *J. Phys. Chem.* **1996**, *100*, 16502.

(35) Wang, H.; Frenklach, M. *J. Phys. Chem.* **1994**, *98*, 11465.

(36) Lee, C. T.; Yang, W. T.; Parr, R. G. *Phys. Rev. B* **1988**, *37*, 785.

(37) Becke, A. D. *J. Chem. Phys.* **1993**, *98*, 5648.

(38) Stewart, J. J. P. Quantum Chemistry Exchange Program No. 455; CS ChemBats3D Pro 4.0, CambridgeSoft, Cambridge, MA, 1997 ed.; Indiana University: Bloomington, IN, 1983.

(39) Frisch, M. J.; Trucks, G. W.; Schlegel, H. B.; Scuseria, G. E.; Robb, M. A.; Cheeseman, J. R.; Zakrzewski, V. G.; Montgomery, J. A., Jr.; Stratmann, R. E.; Burant, J. C.; Dapprich, S.; Millam, J. M.; Daniels, A. D.; Kudin, K. N.; Strain, M. C.; Farkas, O.; Tomasi, J.; Barone, V.; Cossi, M.; Cammi, R.; Mennucci, B.; Pomelli, C.; Adamo, C.; Clifford, S.; Ochterski, J.; Petersson, G. A.; Ayala, P. Y.; Cui, Q.; Morokuma, K.; Malick, D. K.; Rabuck, A. D.; Raghavachari, K.; Foresman, J. B.; Cioslowski, J.;

Ortiz, J. V.; Stefanov, B. B.; Liu, G.; Liashenko, A.; Piskorz, P.; Komaromi, I.; Gomperts, R.; Martin, R. L.; Fox, D. J.; Keith, T.; Al-Laham, M. A.; Peng, C. Y.; Nanayakkara, A.; Gonzalez, C.; Challacombe, M.; Gill, P. M. W.; Johnson, B. G.; Chen, W.; Wong, M. W.; Andres, J. L.; Head-Gordon, M.; Replogle, E. S.; Pople, J. A. *Gaussian 98*, revision A.9; Gaussian, Inc.: Pittsburgh, PA, 1998.

(40) Dewar, M. J. S.; Zoebisch, E. G.; Healy, E. F.; Stewart, J. J. P. *J. Am. Chem. Soc.* **1985**, *107*, 3902.

(41) Benson, S. W. *Thermochemical Kinetics*, 2nd ed.; Wiley: New York, 1976.

(42) Sarobe, M.; Jenneskens, L. W.; Kleij, A.; Petroutsa, M. *Tetrahedron Lett.* **1997**, *38*, 7255.

(43) Frenklach, M.; Moriarty, N. W.; Brown, N. J. *Proc. Combust. Inst.* **1998**, *27*, 1655.

(44) Sarobe, M.; Jenneskens, L. W.; Steggink, R. G. B.; Visser, T. *J. Org. Chem.* **1999**, *64*, 3861.

(45) Grieco, W. J.; Lafleur, A. L.; Swallow, K. C.; Richter, H.; Taghizadeh, K.; Howard, J. B. *Proc. Combust. Inst.* **1998**, *27*, 1669.

(46) Marr, J. A.; Giovane, L. M.; Longwell, J. P.; Howard, J. B.; Lafleur, A. L. *Combust. Sci. Technol.* **1994**, *101*, 301.

(47) Badger, G. M.; Donnelly, J. K.; Spotswood, T. M. *Aust. J. Chem.* **1964**, *17*, 1147.

(48) Wornat, M. J.; Lafleur, A. L.; Sarofim, A. F. *Polycyclic Aromat. Compd.* **1993**, *3*, 149.